

A STUDY ON SEISMIC SSI ANALYSIS OF A BASE-ISOLATED STORAGE STRUCTURE FOUNDED ON FIRM SOIL

Dan M. Ghiocel¹, Victor Kostarev², Alex Kultsep³ and Peter Nawrotzki⁴

¹ President, Ghiocel Predictive Technologies, Inc., New York, USA (dan.ghiocel@ghiocel-tech.com)

² President, CKTI-Vibroiseism, Saint-Petersburg, Russia (victor.kostarev@gmail.com)

³ Principal, CKTI-Vibroiseism, Saint-Petersburg, Russia (alex.kultsep@cvs.spb.ru)

⁴ Director, GERB Vibration Control Systems, Berlin/Essen, Germany (peter.nawrotzki@gerb.de)

ABSTRACT

The paper investigates the seismic SSI effects for a base-isolated reinforced concrete (RC) storage structure founded on firm soil. Three types of base-isolators are considered: 1) Lead-Rubber Bearing (LRB) isolators, 2) Triple Pendulum Friction (TPB) and 3) Base Control System (BCS) isolators including a combination of spring units and high-viscosity damper units. Two level of earthquake severity are considered: 1) 0.40g for DBE and 2) 0.60g for BDBE (1.5 DBE). Both deterministic and probabilistic simulations are considered. The paper also investigates the effects of motion incoherency on the SSI responses for base-isolated structure and shows that these effects are quite significant. The LRB and TPB isolators are modelled as hysteretic systems, while the BCS isolators are modelled using a combination of linear springs and frequency-dependent 3D high-viscosity damper (HVD) systems. Results highlight the significant additional benefits of the 3D-space BCS in comparison with the traditional 2D-space horizontal LRB and TPB systems, for reducing of the large structural amplifications due local vibration modes, reducing drastically the floor vertical vibrations, totally filtering out the detrimental amplifications due to the motion incoherency effects, and also reducing the structural moments more significantly than the other isolation systems.

INTRODUCTION

To perform the deterministic and probabilistic nonlinear seismic SSI analyses for the base-isolated auxiliary storage (AS) structure for the hysteretic LRB and TPB isolators, the ACS SASSI NQA software with advanced options PRO (probabilistic SSI) and NON (nonlinear hysteretic isolators) capabilities was used (GP Technologies, 2022). The ACS SASSI NQA also includes specialized frequency-dependent HVD finite elements that are defined as a combination of two parallel Maxwell chains (with 3-nodes each) including a total of four input parameters (Ghiocel, 2019, Kostarev et al., 2019, Nawrotzki et al., 2019).

AUXILIARY STORAGE (AS) STRUCTURE MODEL

The two-level hypothetical AS structure FE model used in this study is shown in Figure 1. The structure has a square shape in horizontal plane with a size of 48m x 48m, and height of 22.5m. The total AS structure weight is 48, 315 tons. The AS structure is like a stiff concrete box with four exterior walls including inside a separation wall and three frame structures for supporting the moving cranes in X-direction. The frames are designed to be not connected to the building exterior walls.

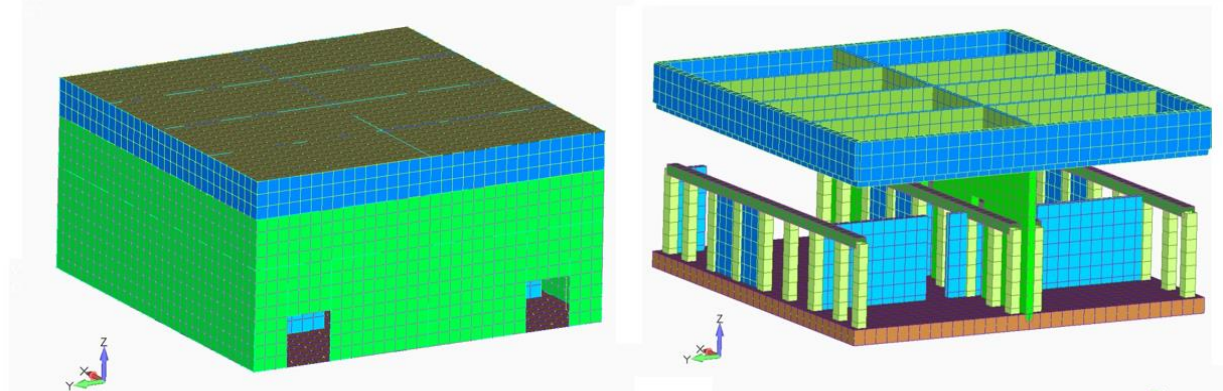


Figure 1 AS Structure FE Model; Exterior View (left) and Interior View (right)

The AS concrete box structure is very stiff with horizontal and vertical natural vibration frequencies above 10 Hz. However, the internal crane frames are more flexible having transversal vibration modes in Y-direction at about 4.4 Hz and 6.9 Hz frequencies.

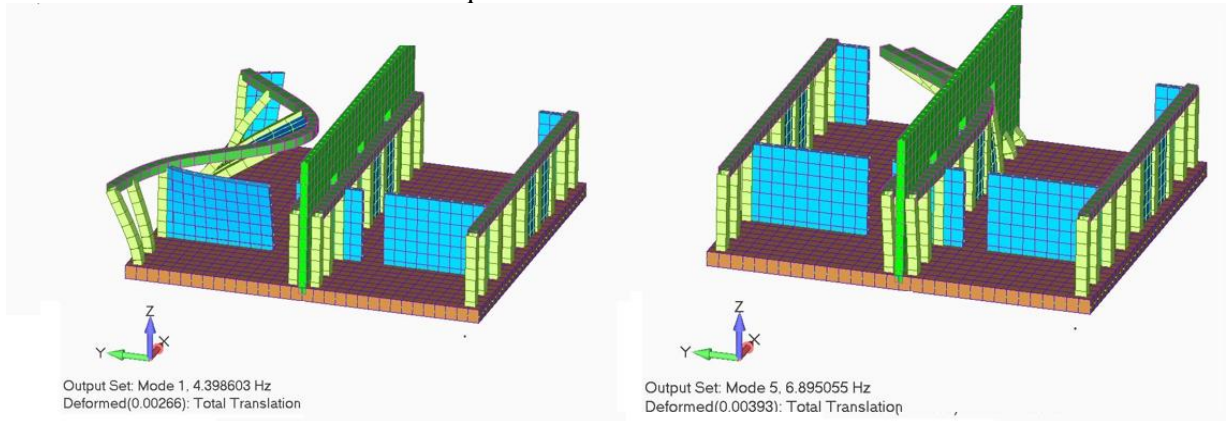


Figure 2 Transverse Vibration Modes of Crane Frames in Y-Direction

BASE ISOLATOR INPUT DATA

The isolators were uniformly distributed on the foundation mat area. A total of 121 isolators were considered equally spaces on a grid of 11 x 11 for all bearing types.

Lead-Rubber Bearing (LRB) Isolators

121 Bridgestone LH070G4 devices were selected. The LRB were modeled using nonlinear shear springs for horizontal direction, and very stiff linear axial springs for vertical direction. For nonlinear springs a set of back-bone curves (BBC) were defined for horizontal spring force as function of horizontal displacement. The characteristic parameters of the BBC are provided in Figure 3.

Do (mm)	Outer diameter	700
Kd (N/mm)	Post-yield stiffness	740.45
Qd (N)	Characteristics strength	62486
K1 (N/mm)	Initial stiffness	9625.8
Kv (N/mm)	Compressive stiffness	2243484.0

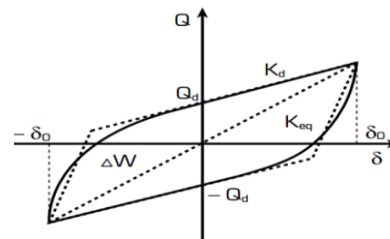


Figure 3. LRB Isolator Back-Bone Curve and Hysteretic Loop for Cyclic Motion

Triple Pendulum Bearing (TPB) Isolators

121 Standard TPB isolators were selected as shown in Figure 4 (Fenz and Constantinou, 2008). The TPB were modeled using nonlinear shear springs for horizontal direction, and very stiff linear axial springs for vertical direction. For nonlinear springs a set of back-bone curves (BBC) were defined for horizontal spring force depending on horizontal displacement. The BBC data is provided in Figure 5.

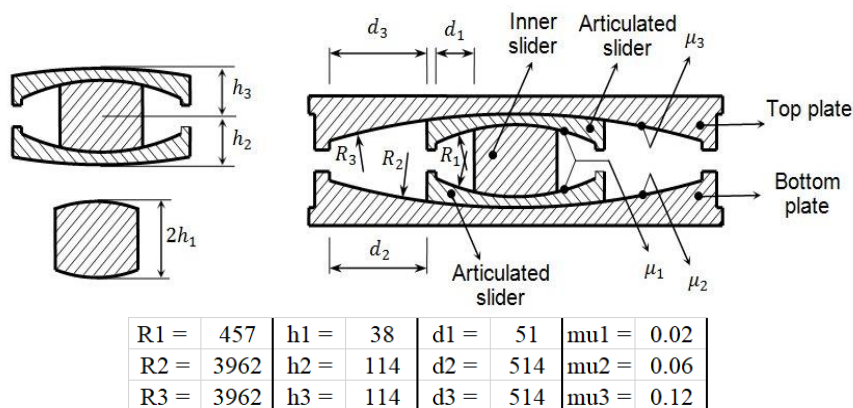


Figure 4 Standard TPB Isolator Characteristics

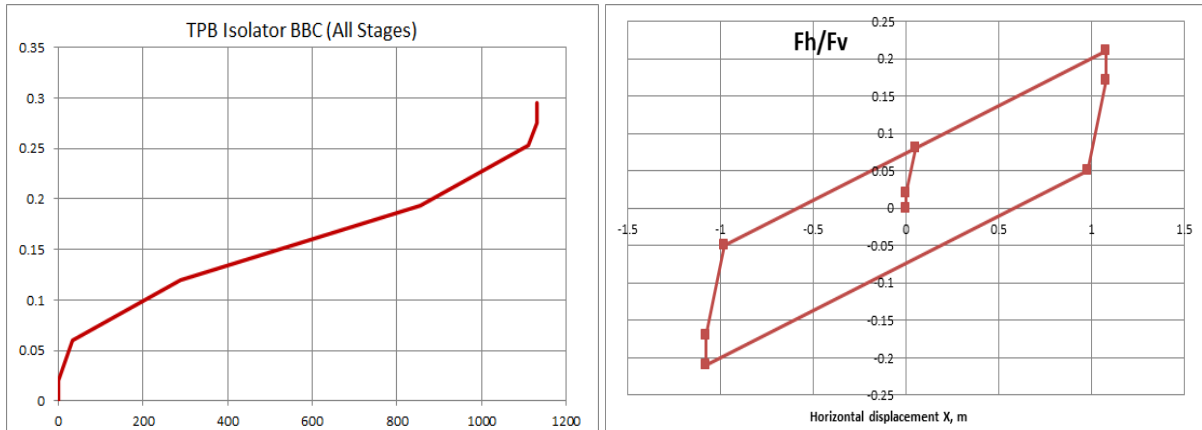


Figure 5 TPB Isolator Back-Bone Curve (All Stages) and Hysteretic Loop for Given Cyclic Amplitude

It should be noted that the BBC is a normalized curve to the vertical axial load in isolators, herein assumed to be constant and produced by the gravity load. The nonlinear spring modeling is simplified since it does not capture the TPB pendulum effects due to the concave geometry of the friction surfaces and friction dependency on instant force and velocity, which are expected to produce some high-frequency vibration components and tendency to uplift as shown against experiments (Fenz and Constantinou, 2008).

Base Control System (BCS) Isolators

121 FE-NI-BCS-02.2 GERB Spring Blocks modeled by linear axial spring elements and 121 viscous dampers modeled by frequency-dependent HVD elements. Dampers are placed nearby of spring blocks.

Type	Capacity (MN)	Kh (kN/mm)	Kv (kN/mm)	Static deflection under dead load (mm)	Limit horizontal displacement (mm)
FE-NI-BCS-02.2	3.85	6.65	71	50.1	150

The HVD unit properties (4 parameter Maxwell model with 2 chains) are as follows;

Type	Kh1 (kN/mm)	Kh2 (kN/mm)	Ch1 (kNs/m)	Ch2 (kNs/m)
VDVL-850/500/437-145/95-11 RHY	64.6	54.0	738.1	6372.0
	Kv1 (kN/mm)	Kv2 (kN/mm)	Cv1 (kNs/m)	Cv2 (kNs/m)
	58.0	24.6	549.1	1899.4

SEISMIC SSI ANALYSIS INPUTS

For the seismic DRS input is shown in Figure 6 was used for deterministic analysis and probabilistic analysis for BDBE level with 0.60g for horizontal directions and 0.40g for vertical direction. For DBE level, the DRS was scaled to 0.40g for horizontal and 0.27g for vertical direction. The soil condition was defined by a deep soil deposit with $V_s=600$ m/s. For the 60 probabilistic DRS simulations, the lognormal distribution was assumed and a c.o.v. of 20% was considered. For the 60 probabilistic V_s profiles, the lognormal distribution was assumed and a c.o.v. of 22% was considered. No probabilistic variations are considered for structure.

For the LRB and TPB hysteretic isolators, nonlinear SSI analysis was performed with the ACS SASSI Option NON software (GP Technologies, 2022) using nonlinear springs for isolator behavior modeling. Figure 7 shows two typical LRB and TPB isolator shear force hysteretic responses for the base-isolated AS structure for the 0.40g DBE input. The TPB isolators behave much stiffer than the LRB isolators.

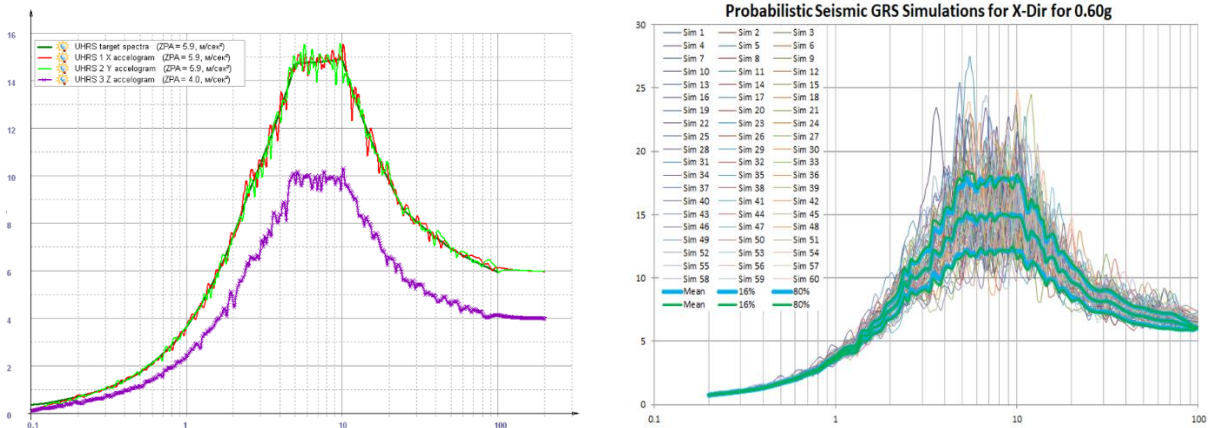


Figure 6 Seismic DRS Input Scaled at 0.60g; Deterministic (left) and Probabilistic (right) w/ 60 Samples

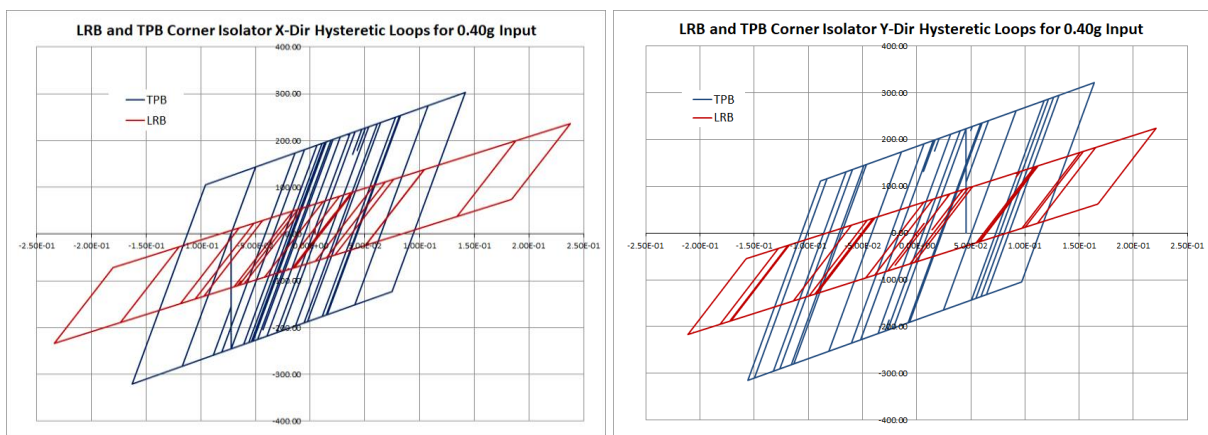


Figure 7 Nonlinear LRB and TPB Isolator Responses for X and Y Directions

SEISMIC SSI RESPONSES FOR COHERENT SEISMIC INPUT

The seismic SSI analyses were performed for the AS structure sitting on LRB, TPB or BCS isolators, and, for comparison, on perfectly rigid isolators. Figure 8 shows the selected seismic response locations. To investigate the AS structure motion, four node locations, specifically, nodes 803, 2620, 2640 and 4459, were considered (left). For evaluating the efficiency of base-isolation on reducing structural forces, two columns of a crane frame were selected (right).

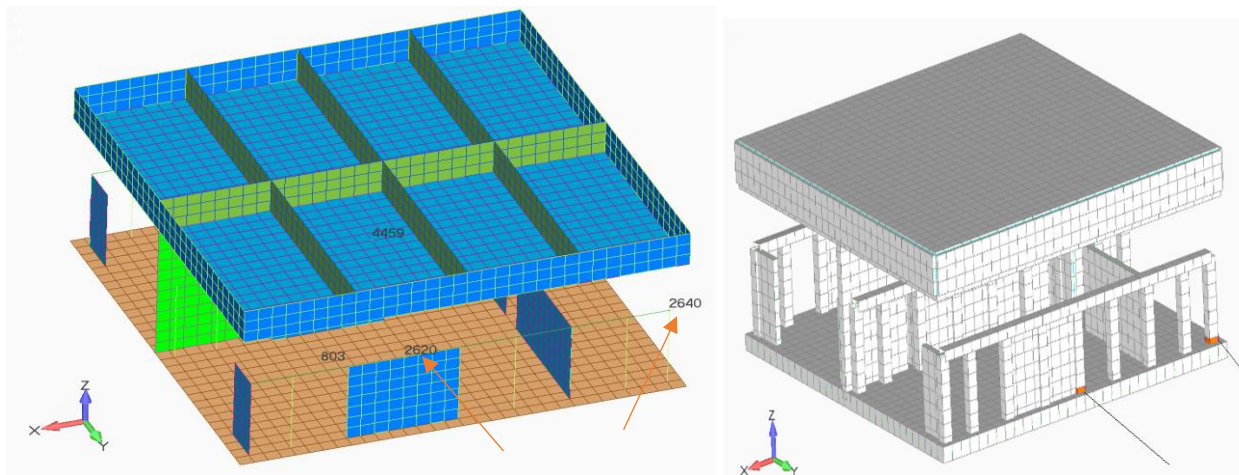


Figure 8 Outputs for SSI Response; Four Node Locations (left) and Two Base Columns (right)

Since the frame is along the X-direction, it is expected that large amplification local vibration modes will manifest in Y-direction (see also Figure 2).

Figures 9 and 10 shows computed ISRS at the top basemat above isolators (Node 803) and roof level (Node 4459) for 0.40g horizontal input. Nodes 803 and 4456 are on the AS main box structure. Computed results include the deterministic ISRS for LRB, TPB, BCS and Rigid isolators, but also the probabilistic simulation-based ISRS computed for the mean and 80% non-exceedance probability (NEP).

Figure 9 shows the top base ISRS for X-horizontal and Z-vertical directions. It should be noted that for horizontal direction the LRB isolators are the softest isolators, while the BCS isolators are the stiffest isolators. The ISRS amplitude reduction factors for the horizontal ISRS at the top basemat is about 2 for BCS and about 5 for LRB and TPB. For vertical ISRS, there is a 15-20% amplitude amplification for all LRB, TPB and BCS. The BCS isolators show a substantial reduced isolator stiffness in vertical direction in comparison the LRB and TPB isolators.

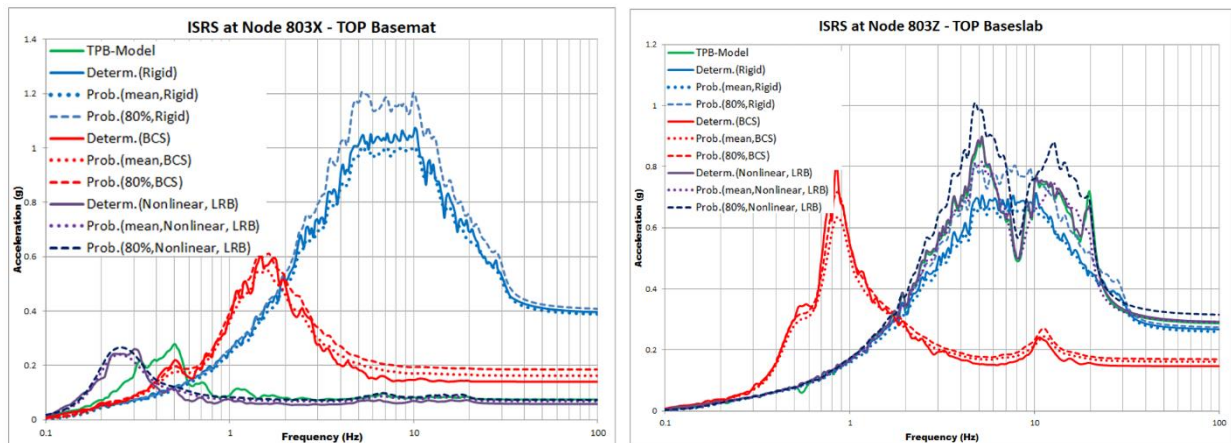


Figure 9 Comparative ISRS for Top Basemat Location (Node 803) in X and Z Directions

Figure 10 shows the roof ISRS for ISRS for Y-horizontal (left) and Z-vertical (right) directions. It should be noted the large benefit from all isolators for reduction the horizontal ISRS amplitudes. For the vertical direction, the BCS isolators are much more efficient since they reduce the floor vibration by few times more than the LRB isolators. From Figure 10, there is another aspect to be remarked, that the probabilistic-based mean and 80% NEP horizontal ISRS are significantly larger that the deterministic ISRS. However, herein, the deterministic ISRS was computed only for a single BE soil profile, not as an envelope of three ISRS for BE, LB and UB soils. If the 80% NEP ISRS are considered for deterministic design of base-isolated structures as discussed in ASCE 4-16 Chapter 1 Commentary, then, using multiple randomized seismic inputs simulations, as recommended in ASCE 4-16 Chapter 12, appears to be strongly justified.

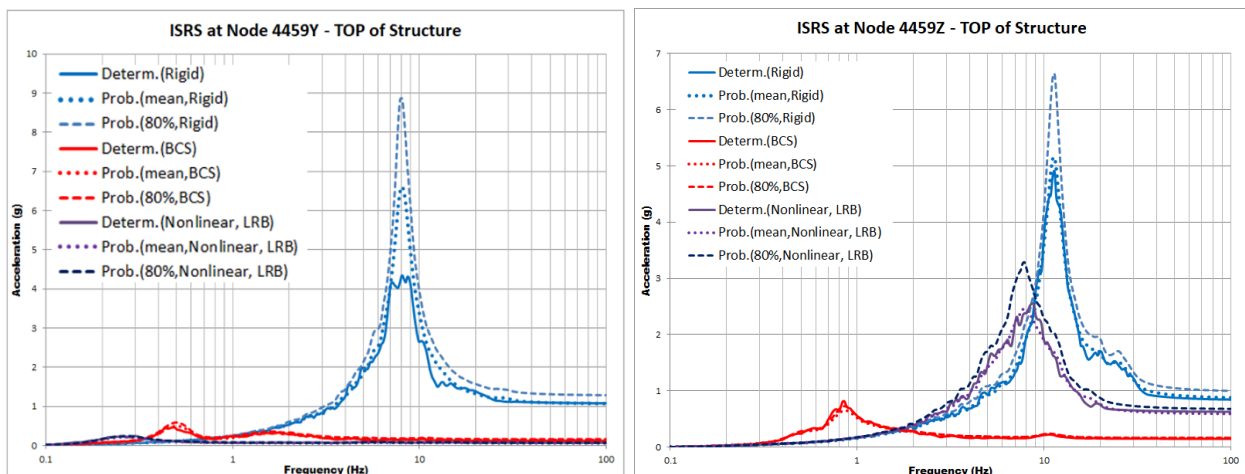


Figure 10 Comparative ISRS for Top Floor (Roof) Location (Node 4459) in X and Z Directions

As a note, it should be understood that the BCS system behavior can be significantly improved if the viscous damper units are placed denser on the basemat perimeter to damp the rocking motion. Herein, as the initial part of the study, we considered the viscous dampers spatially uniformly distributed on the basemat.

Figure 11 shows the AS structure motion (frozen at a given time step) for the LRB (left) and BCS (right) base isolators under seismic coherent inputs. External walls are not shown. It should be noted that using the BCS isolators, there is basically no transmission of the basemat deformation into the structure. The BCS isolated structure moves a rigid body. However, this BCS rigid body behavior is only possible since the BCS vertical stiffness is much softer than the LRB vertical stiffness.

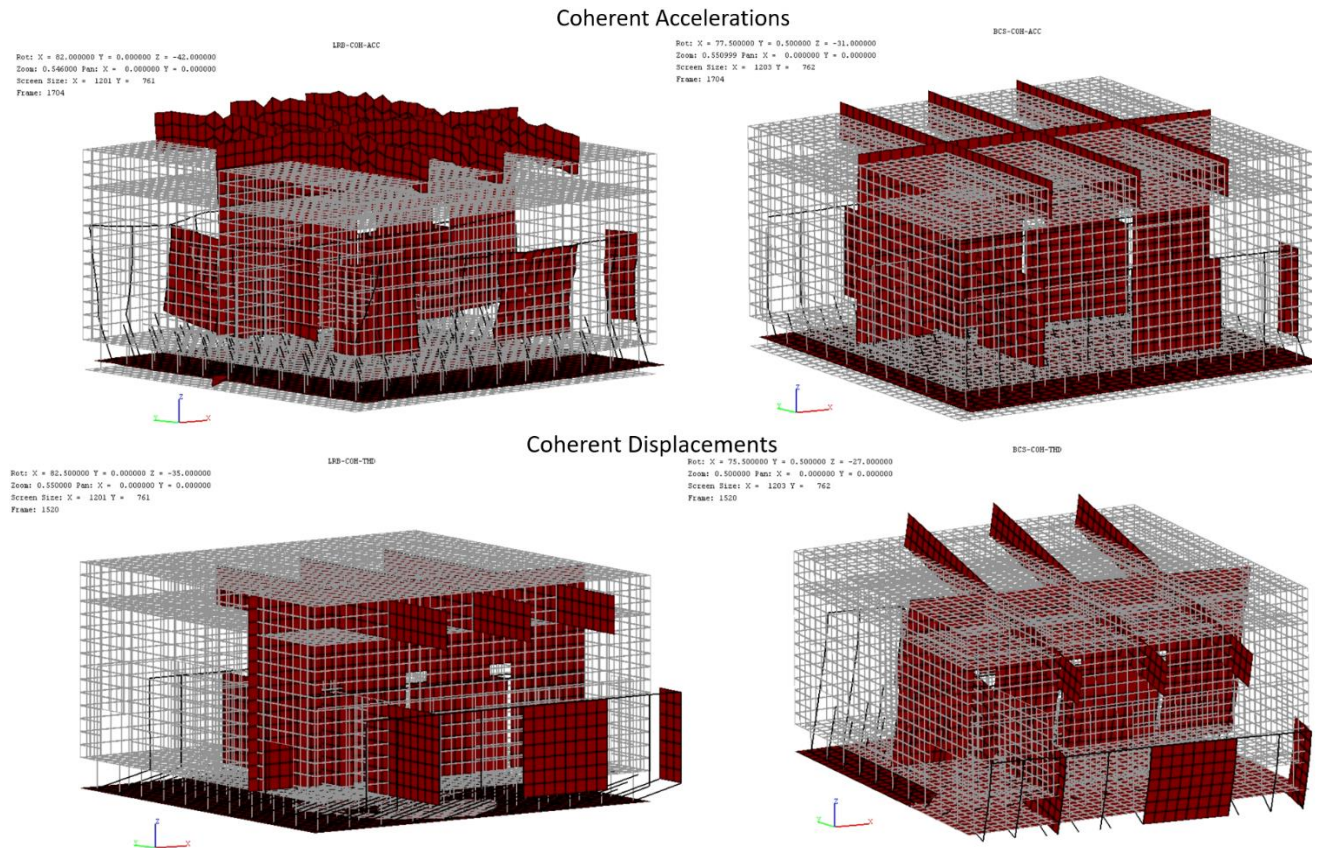


Figure 11 LRB (left) and BCS (right) Isolated AS Structure Motion at Given Time; Acceleration (upper) and Displacements (lower)

Figures 12 and 13 show the ISRS on the top of the selected crane frame in the Y-transverse direction, at nodes 2620 and 2640 (see Figure 8 right for node locations). The left plots include the Rigid isolator case.

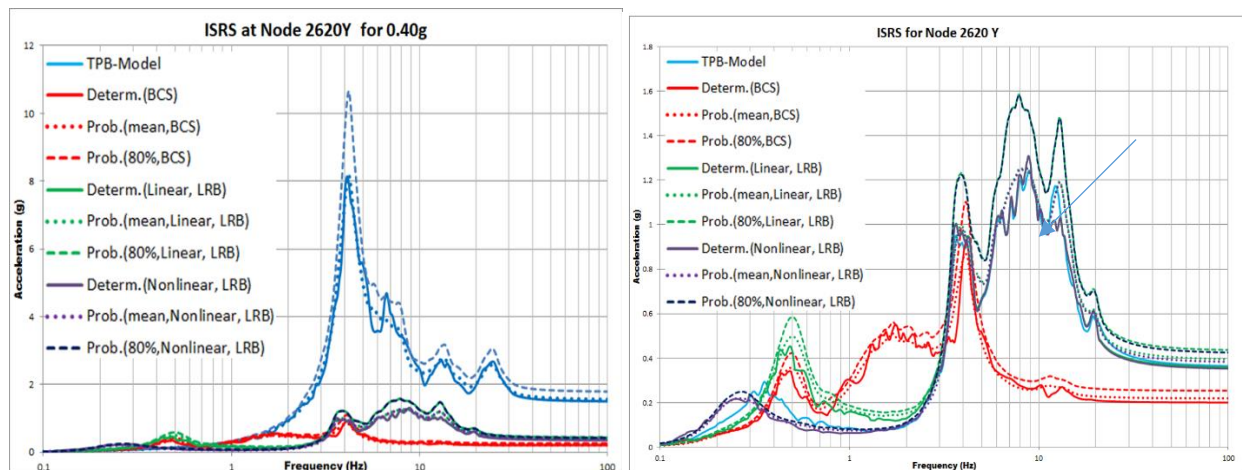


Figure 12 Comparative ISRS for Crane Frame Location (Node 2620) in Y Direction

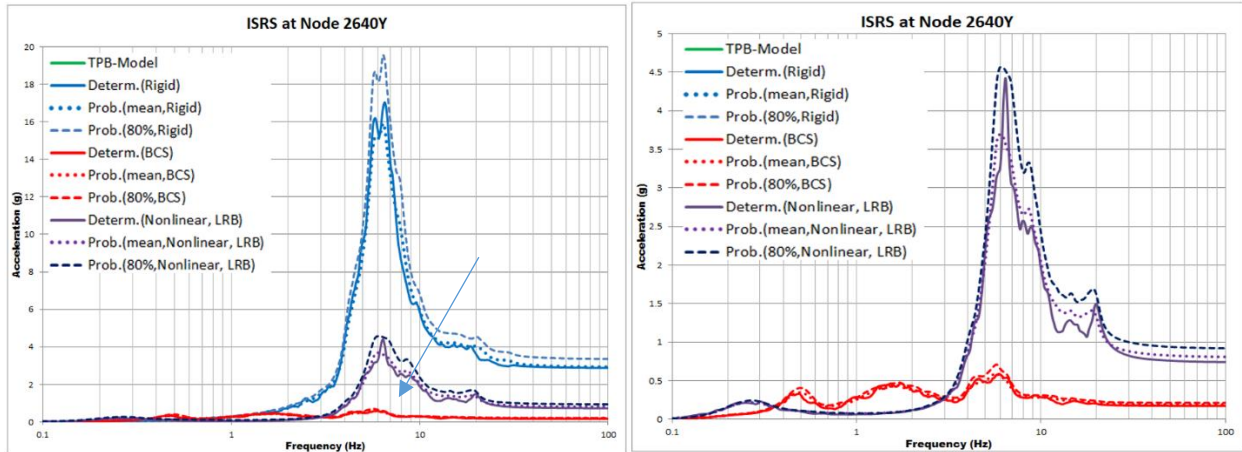


Figure 13 Comparative ISRS for Crane Frame Location (Node 2640) in Y Direction

In comparison with the Rigid isolator case, all isolator types, perform very well providing a deterministic ISRS peak reduction of at least 4 times for the 2640 node location, and 5-6 times for the 2620 node location. However, Figure 13 indicate that for the local vibration modes of the crane frame, the BCS isolators significantly outperforms the LRB and TPB isolators. For BCS isolators the 2640Y ISRS reduction is about 32 times, in comparison with LRB isolators for which 2640Y ISRS reduction is only 4 times, so that the ISRS peak has still a high amplitude of 4.5g.

Table 1 is a summary for the base-isolated AS structure displacement with respect to the bottom basemat center location below isolators. Both 0.4g and 0.6g input levels are included. As expected, the table results indicate for the BCS isolators smaller horizontal displacement amplitudes and much larger vertical displacement amplitudes. At the top basemat level, above isolators, the BCS horizontal displacement amplitude is 30.38 mm, which is about 6 times smaller than LRB and 3.3 times smaller than TPB isolators.

Table 1 Base-Isolated AS Structure Deterministic Maximum Displacement With Respect to Bottom Basemat center (Below Isolators)

		0.40g			0.60g		
		Bottom Base Center Node			Bottom Base Center		
	Nodel	Dx(mm)	Dy(mm)	Dz(mm)	Dx(mm)	Dy(mm)	Dz(mm)
RIGID	803	0.0035	0.0027	0.0056	0.0053	0.0041	0.0083
	2620	0.6964	18.6857	0.1118	1.0441	28.0265	0.1671
	2640	1.0255	19.3032	0.0162	1.5381	28.9569	0.0242
	4459	2.9373	4.156	1.6635	4.406	6.2341	2.4674
BCS	803	30.376	25.959	69.1061	45.5646	38.9384	103.62
	2620	68.1378	64.5371	115.725	102.203	96.8021	173.587
	2640	68.1556	61.7176	126.201	102.23	92.5774	188.892
	4459	102.083	89.5653	57.0814	153.119	134.348	85.376
LRB	803	186.069	219.186	0.1545	363.533	290.888	0.2372
	2620	189.54	220.369	1.0024	364.324	295.375	1.3273
	2640	189.571	219.088	1.2349	364.413	289.014	1.8044
	4459	186.818	219.819	2.4651	364.513	291.556	3.2872
TPB	803	102.238	130.002	0.1655	367.767	634.614	0.3004
	2620	101.043	131.044	0.9177	368.267	645.439	1.6489
	2640	101.087	125.047	1.1455	368.357	652.9	2.4333
	4459	102.589	129.739	2.2001	368.935	639.16	3.339

Table 2 shows the deterministic maximum moments computed in the two frame crane columns (see Figure 8 right) for 0.40g and 0.60g seismic input. Table 2 results indicate the efficiency of base isolation to reduce

structural component forces (kN) and moments (kN-m). The maximum largest moment M3 reduction factors are in the range of 6.2-15.2 for BCS, 5.1-6.7 for LRB and 5-6.1 for TPB.

Table 2 Base-Isolated AS Structure Crane Frame Column Deterministic Maximum Moments

		0.4g						0.6g					
		Point 1 (Element 190)						Point 2 (Element 224)					
		M1 TORSION SIS effect,		M2 SIS effect,		M3 SIS effect,		M1 TORSION SIS effect,		M2 SIS effect,		M3 SIS effect,	
Model	Node #	Mt, kN	times=	Mt, kN	times=	Mt, kN	times=	Mt, kN	times=	Mt, kN	times=	Mt, kN	times=
RIGID	59 (Node	7.9		734.9		4360.5		11.8		1102.1		6540.6	
	1148 (No	7.9		544		3378		11.8		815.8		5066.8	
	1129 (No	146.8		103.2		2786.2		220.2		154.8		4179	
	40 (Node	146.8		496.7		2925.4		220.2		744.8		4387.7	
BCS	59 (Node	0.7	11.3	195	3.8	313	13.9	1.1	10.7	292.2	3.8	469.3	13.9
	1148 (No	0.7	11.3	131.9	4.1	221.8	15.2	1.1	10.7	197.7	4.1	332.6	15.2
	1129 (No	29.8	4.9	43.3	2.4	427.3	6.5	44.7	4.9	64.9	2.4	640.5	6.5
	40 (Node	29.8	4.9	164	3.0	475.1	6.2	44.7	4.9	245.8	3.0	712.2	6.2
LRB	59 (Node	2.2	3.6	117.7	6.2	897.7	4.9	3.2	3.7	170.6	6.5	1294	5.1
	1148 (No	2.2	3.6	82.9	6.6	668.4	5.1	3.2	3.7	120.2	6.8	975.1	5.2
	1129 (No	35.9	4.1	26.2	3.9	450.2	6.2	51.8	4.3	37.3	4.2	642.7	6.5
	40 (Node	35.9	4.1	69.7	7.1	457.7	6.4	51.8	4.3	100.2	7.4	655.3	6.7
TPB	59 (Node	2.2	3.6	142	5.2	890.7	4.9	3.3	3.6	189.1	5.8	1310.3	5.0
	1148 (No	2.2	3.6	94.7	5.7	667.6	5.1	3.3	3.6	130.6	6.2	984.1	5.1
	1129 (No	39	3.8	32.8	3.1	493	5.7	56	3.9	44.2	3.5	705.8	5.9
	40 (Node	39	3.8	75.8	6.6	498.2	5.9	56	3.9	109.6	6.8	714.1	6.1

Table 3 shows the deterministic maximum forces (kN) in isolators, including the Rigid isolator case as a reference case. It should be noted that the largest forces are in the corner isolators at the node 121. The BCS isolators, as expected, provide the maximum isolation benefits reducing the maximum isolator forces by about three times in comparison with the LRB and TPB isolators.

Table 3 Maximum Seismic Forces in the AS Structure Base-Isolators

		0.4g			0.6g		
Model	Element #	Axial Force Z	Shear Force X	Shear Force Y	Axial Force Z	Shear Force X	Shear Force Y
RIGID	Corner Element 1	8847.2	2718.2	8710	13270.6	4076.3	13065.7
	Centerr Element 61	9175.5	2016	9522.7	13760.9	3024	14283.5
	Corner Element 121	27993	4533	32066.3	41973	6769.8	48093.8
BCS	Corner Element 1	203.2	196	203.1	304.7	294	304.7
	Centerr Element 61	181.9	179.1	183.5	272.8	268.7	275.3
	Corner Element 121	974.1	299.1	1034.6	1459.3	443.3	1550.1
LRB	Corner Element 1	204.9	204.5	205.2	40.5	40.4	40.5
	Centerr Element 61	233	235.2	238.6	33.4	33.6	33.9
	Corner Element 121	3252	2034.4	3460.6	4833	2981.4	5128.8
TPB	Corner Element 1	238.6	249.8	260.6	563.2	562.8	563.4
	Centerr Element 61	226.3	227.8	236.1	1068	1054	1043
	Corner Element 121	3216.9	2012.6	3416.7	5342.3	2981.8	5772.1

COMPARATIVE RESPONSES UNDER COHERENT AND INCOHERENT INPUTS

In this section, the effects on motion incoherency on the base-isolated AS structure are investigated for the 0.40g seismic input. To model motion incoherency the Abrahamson coherence function for soil condition was applied (Abrahamson, 2007). For incoherent SSI analysis, the Stochastic Simulation approach implemented in ACS SASSI with five incoherent motion simulations was used to compute the average incoherent seismic responses. Only the LRB and BCS isolators are included.

Figure 14 shows the effects of motion incoherency on the ISRS computed at the top basemat above isolators, node 803. The left plots include the Rigid isolator case. For the X-horizontal direction, it should be noted that for LRB isolators the incoherent ISRS is highly amplified in comparison with coherent ISRS. The incoherent ISRS amplification corresponds to the dominant frequency range of the seismic input

motion. However, for the BCS isolators this ISRS discrepancy due to incoherency effects is not visible. The vertical ISRS show not much effects of motion incoherency.

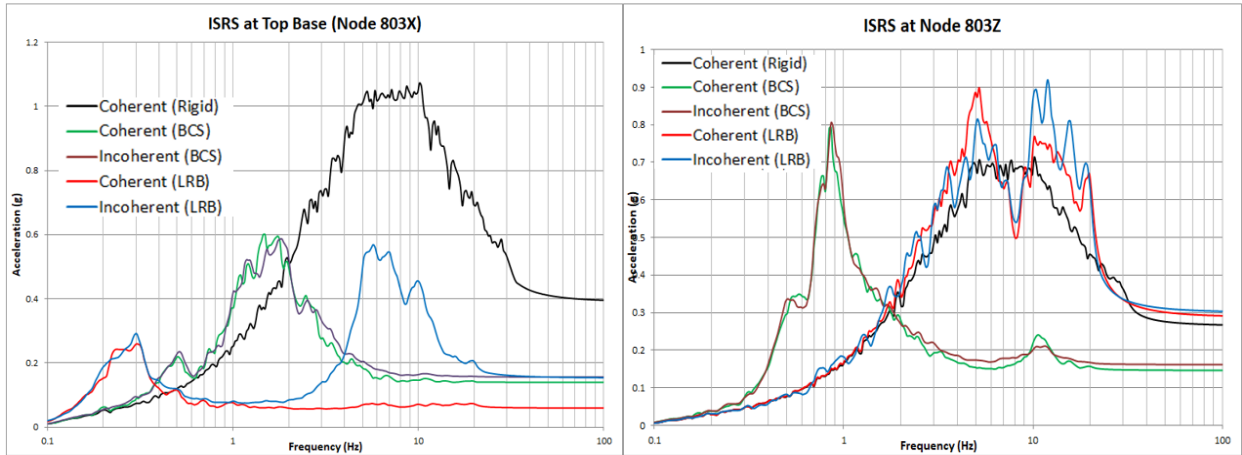


Figure 14 Comparative ISRS for Top Basemet Location (Node 803) in X and Z Directions

Figure 15 show the computed ISRS for roof level, node 4459 in X-direction. Left plots include the Rigid isolators case, while right plots do not include this case. Same incoherency effects as shown in Figure 14.

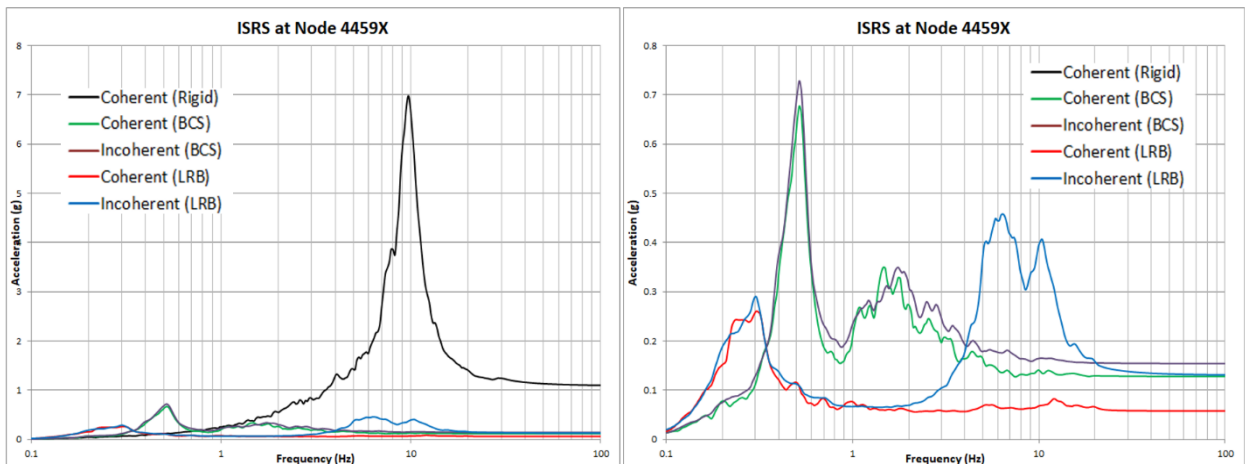


Figure 15 Comparative ISRS for Top Floor (Roof) Location (Node 4459) in X and Z Directions

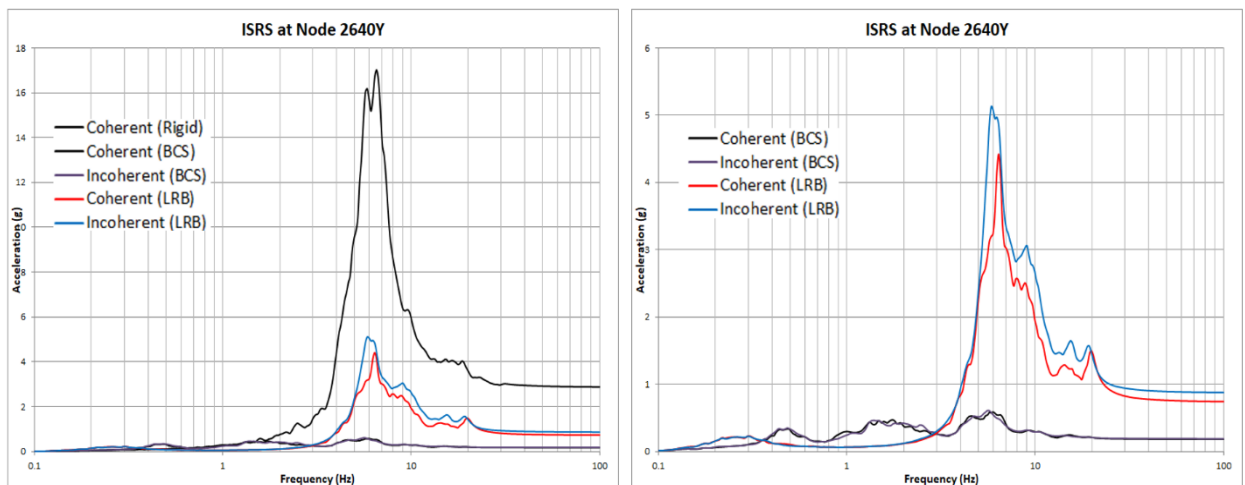


Figure 16 Comparative ISRS for Crane Frame Location (Node 2640) in Y Direction

Figure 16 shows the motion incoherency effects on the crane frame ISRS which is dominated by the local transverse vibration in Y-direction.

The BCS isolators again, under incoherent inputs, totally cut the ISRS amplification due to local vibration mode. This is a notable performance. The LRB isolators amplify slightly higher the horizontal ISRS due to the local mode effects under the incoherent inputs.

Figures 17 and 18 show for crane frame locations all the five incoherent ISRS simulations in comparison with coherent ISRS. The LRB results are shown in left plots, while the BCS results are shown in right plots.

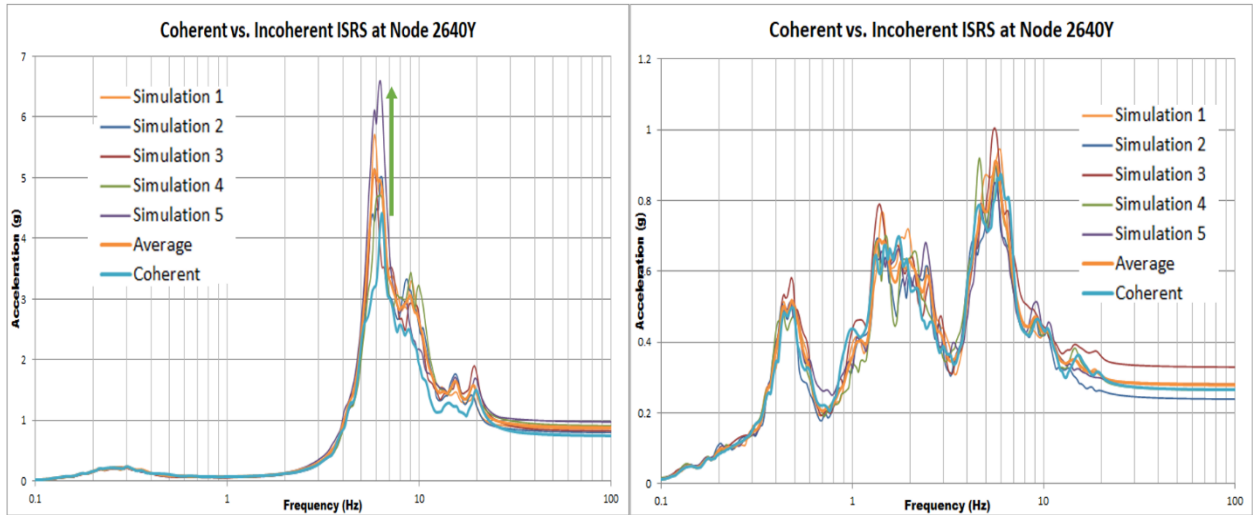


Figure 17 Incoherent ISRS Simulations for LRB and BCS Crane Frame Location (Node 2640) in Y Dir

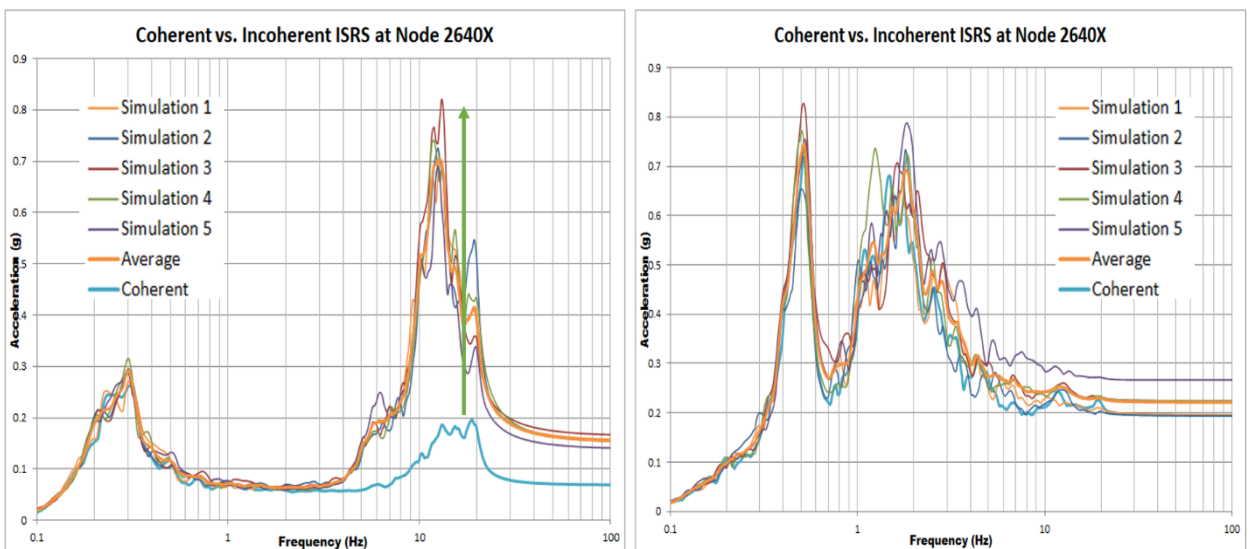


Figure 18 Incoherent ISRS Simulations for LRB and BCS Crane Frame Location (Node 2640) in X Dir

The green arrows in the LRB plots in Figures 17 and 18 show the ISRS spectral amplification due to motion incoherency effects. It should be noted that the BCS ISRS plots shows no visible ISRS amplification due to motion incoherency effects.

The effect of motion incoherency on AS structure response is visualized in Figures 19 and 20. Figure 19 shows the instant structural accelerations for LRB isolators for coherent (left) and incoherent (right) inputs. Apparently, there is a visible more global deformation of the AS structure due to incoherency.

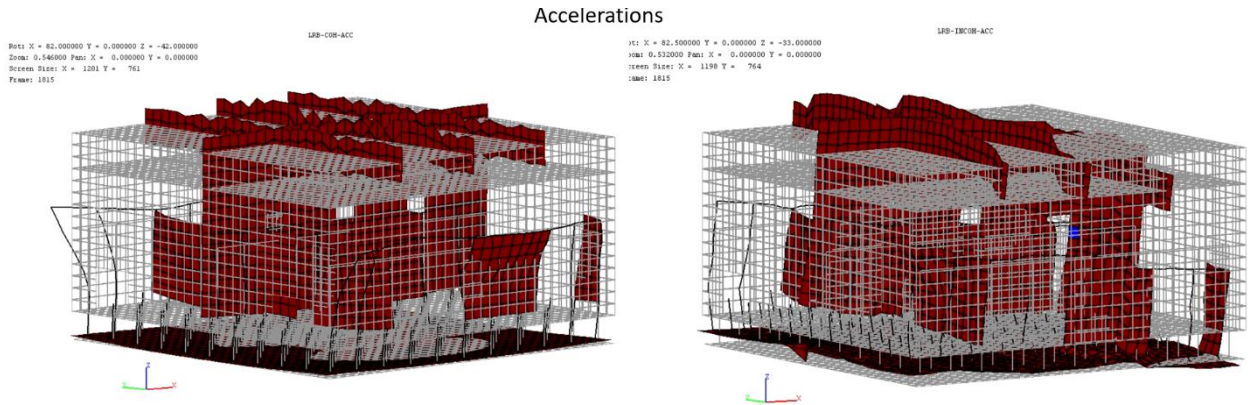


Figure 19 LRB Isolator Coherent (left) and Incoherent (right) Response Accelerations at Given Time; Figure 20 shows the instant structural accelerations for BCS isolators for coherent (left) and incoherent (right) motion inputs. Apparently, there is no deformation of the AS structure due to incoherency.

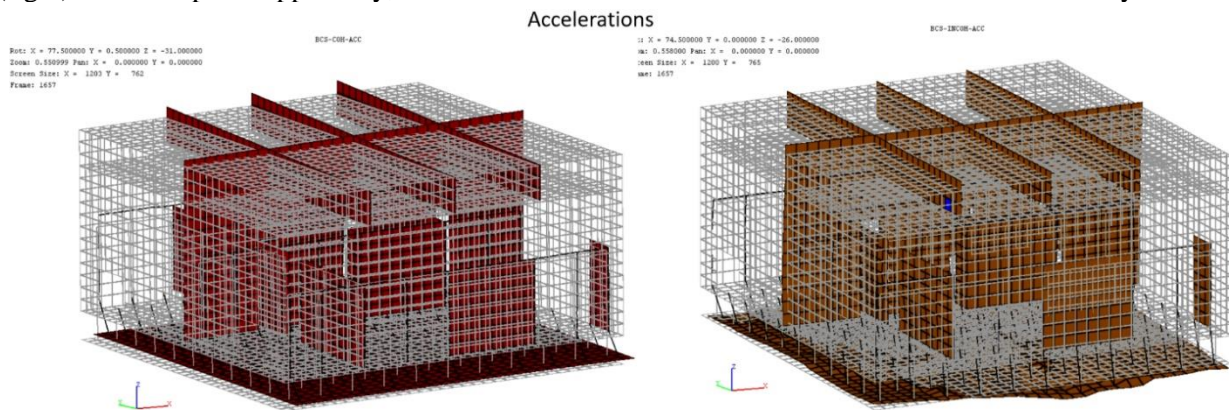


Figure 20 BCS Isolator Coherent (left) and Incoherent (right) Response Accelerations at Given Time;

CONCLUDING REMARKS

The study results for the AS structure indicate significant benefits of the application of the 3D-space BCS isolation system in comparison with the traditional 2D-space horizontal LRB and TPB isolation systems. The BCS isolator system additional benefits in comparison with LRB and TPB systems include:

- 1) Reducing drastically the large ISRS amplifications due local vibration of the crane frame,
- 2) Reducing drastically the floor vertical vibrations due to its efficient vertical isolation,
- 3) Completely filtering out the detrimental amplifications due to motion incoherency effects, and
- 4) Reducing the structural base moments more significantly than the other isolation systems,

Future research studies will focus on the optimization of the BCS viscous damper unit distribution and locations with more units close to the perimeter edges of the basemat. An aspect of practical interest is also to improve the numerical modeling of the TPB isolators by including the pendulum effect and variable friction.

REFERENCES

- Abrahamson, N. (2007). *Effects of Spatial Incoherence on Seismic Ground Motions*, Electric Power Research Institute, Palo Alto, CA and US Department of Energy, Germantown, MD, Report No. TR-1015110, December 20
- American Society of Civil Engineers (2017), *Seismic Analysis for Safety-Related Nuclear Structures and Commentary*, ASCE 4-16 Standard
- Fenz, D.M. and Constantinou, M.C. (2008). *Development, Implementation and Verification for Multi-Spherical Sliding Bearings*, Technical Report MCEER-08-0018, University of Buffalo, NY

- Ghiocel, D.M. (2019) *Probabilistic Seismic SSI Analysis Sensitivity Studies for Base-Isolated Nuclear Structures Subjected to Coherent and Incoherent Motions*, the SMiRT25 Conference Proceedings, Division III, Charlotte, NC, August 4-9
- GP Technologies, Inc. (2022). *ACS SASSI Version 4.3 User Manual, Including Advanced Options A-AA, NON, PRO, RVT-SIM and UPLIFT*, Revision 7, Pittsford, New York, January 31.
- Kostarev, V., Nawrotzki, P., Vasilyev, P. and Vayndrakh, M. (2019) *Developing and natural scale testing of the 3D base isolation system*, 16th World Conference on Seismic Isolation. Energy Dissipation and active Vibration Control (16thWCSI), St. Petersburg
- Nawrotzki, P., Siepe, D., and Salcedo. V. (2019). *Seismic protection of NPP structures using 3-D base control systems*. 25th International Conference on Structural Mechanics in Reactor Technology (SMiRT25), Charlotte, NC.